Toxicology Letters 222 (2013) 55–63

Contents lists available at ScienceDirect

Toxicology Letters

journal homepage: www.elsevier.com/locate/toxlet

Multi-platform genotoxicity analysis of silver nanoparticles in the model cell line CHO-K1

Xiumei Jiang[a,b], Rasmus Foldbjerg[b], Teodora Miclaus[c], Liming Wang[a], Rajinder Singh[d], Yuya Hayashi[c], Duncan Sutherland[c], Chunying Chen[a,*], Herman Autrup[b], Christiane Beer[b,**]

[a] National Center for Nanoscience and Technology, Chinese Academy of Science, No. 11, Beiyitiao Zhongguancun, Beijing 100190, China
[b] Department of Public Health, Aarhus University, Bartholins Alle 2, 8000 Aarhus C, Denmark
[c] iNANO, Aarhus University, Gustav Wieds Vej 14, 8000 Aarhus C, Denmark
[d] Cancer Biomarkers and Prevention Group, Department of Cancer Studies and Molecular Medicine, University of Leicester, Leicester LE1 7RH, UK

ARTICLE INFO

Article history:
Received 28 May 2013
Received in revised form 9 July 2013
Accepted 9 July 2013
Available online 18 July 2013

Keywords:
Genotoxicity
Cytotoxicity
Silver nanoparticle
DNA adduct
8-oxodG
Micronucleus assay

ABSTRACT

Investigation of the genotoxic potential of nanomaterials is essential to evaluate if they pose a cancer risk for exposed workers and consumers. The Chinese hamster ovary cell line CHO-K1 is recommended by the OECD for use in the micronucleus assay and is commonly used for genotoxicity testing. However, studies investigating if this cell line is suitable for the genotoxic evaluation of nanomaterials, including induction of DNA adduct and micronuclei formation, are rare and for silver nanoparticles (Ag NPs) missing. Therefore, we here systematically investigated DNA and chromosomal damage induced by BSA coated Ag NPs (15.9 ± 7.6 nm) in CHO-K1 cells in relation to cellular uptake and intracellular localization, their effects on mitochondrial activity and production of reactive oxygen species (ROS), cell cycle, apoptosis and necrosis. Ag NPs are taken up by CHO-K1 cells and are presumably translocated into endosomes/lysosomes. Our cytotoxicity studies demonstrated a concentration-dependent decrease of mitochondrial activity and increase of intracellular reactive oxygen species (ROS) in CHO-K1 cells following exposure to Ag NPs and Ag^+ (0–20 μg/ml) for 24 h. Annexin V/propidium iodide assay showed that Ag NPs and Ag^+ induced apoptosis and necrosis, which is in agreement with an increased fraction of cells in subG1 phase of the cell cycle. Genotoxicity studies showed that Ag NPs but also silver ions (Ag^+) induced bulky-DNA adducts, 8-oxodG and micronuclei formation in a concentration-dependent manner, however, there were quantitative and qualitative differences between the particulate and ionic form of silver. Taken together, our multi-platform genotoxicity and cytotoxicity analysis demonstrates that CHO-K1 cells are suitable for the investigation of genotoxicity of nanoparticles like Ag NPs.

1. Introduction

Advances in nanoscience and technology prompt the production of various kinds of nanomaterials. Due to their unique physicochemical properties, nanomaterials show great potential for biomedical and industrial applications. Interest on interaction studies of nanomaterials and biological systems has been increasing in recent years (Cheng et al., 2013; Zhao et al., 2011). The toxicity of nanomaterials has also led to more and more concerns and a number of studies regarding the toxicity of nanomaterials have been performed (Li et al., 2012; Liu et al., 2011; Meng et al., 2012; Zhou et al., 2012).

Among various kinds of nanomaterials, silver nanoparticles (Ag NPs) are one of the most widely applied nanomaterials in commercial products due to their effective antibacterial activity (Cohen et al., 2007; Fu et al., 2006; Xu et al., 2008). Widespread applications, especially in healthcare products, increase the chances of human exposure to Ag NPs, which has increased concerns regarding the potential adverse effects. Unlike gold nanoparticles, Ag NPs can release Ag^+ due to surface oxidation (Liu and Hurt, 2010). Kittler et al. (2010) showed that the toxicity of Ag NPs increases during storage due to the release of Ag^+, that is considered to be readily bioactive. In accordance with this, we recently showed that the initial Ag^+ fraction of Ag NP suspensions is important as it contributes greatly to the toxicity of Ag NPs *in vitro* (Beer et al., 2011). Studies suggest that the toxicity of Ag NPs are due to a so-called Trojan-horse mechanism where Ag NPs are taken up by the cells accompanied with subsequent intracellular release of Ag^+ thereby leading to cell death (Lubick, 2008). The observed

* Corresponding author. Tel.: +86 10 8254 5560; fax: +86 10 6265 6765.
** Corresponding author. Tel.: +45 8716 8027.
E-mail addresses: chenchy@nanoctr.cn (C. Chen), cbee@mil.au.dk (C. Beer).

0378-4274/$ – see front matter © 2013 Elsevier Ireland Ltd. All rights reserved.
http://dx.doi.org/10.1016/j.toxlet.2013.07.011

toxicity is assumed to be due to the generation of excess free radicals within the cells (Karlsson et al., 2009; Midander et al., 2009) and oxidative stress mediated pathways have been suggested as the main way of Ag NP induced toxicity (Chairuangkitti et al., 2012; Foldbjerg et al., 2009; Hsin et al., 2008). *In vitro* and *in vivo* cytotoxicity and genotoxicity of Ag NPs has been reported in several studies and reviews (Ahamed et al., 2008; AshaRani et al., 2008; Flower et al., 2012; Hackenberg et al., 2011; Kim et al., 2008, 2011, 2012; Lima et al., 2012). Reactive oxygen species (ROS) can induce oxidative DNA damage and several studies demonstrated elevated levels of 8-oxodG in human cancer tissue (Musarrat et al., 1996; Olinski et al., 2003). Another form of DNA damage is the formation of micronuclei. According to the OECD guidelines the Chinese hamster ovary cell line CHO-K1 is one of the recommended cell lines for the standardized investigation of micronucleus formation (OECD Guidelines for the Testing of Chemicals Test No. 487: *In Vitro* Mammalian Cell Micronucleus Test). However, CHO-K1 cells are rarely used for toxicity studies on nanoparticles and cytotoxicity studies in relation to the formation of micronuclei and DNA adducts, especially oxidative DNA damage products like 8-oxodG, and in the case of Ag NPs presently missing. Therefore, we here systematically investigated the genotoxicity of Ag NPs and Ag^+ in relation to their cytotoxicity to investigate the suitability of CHO-K1 cells for the investigation of the genotoxicity of nanoparticles. Based on the experimental results, a mechanism for the toxicity of Ag NPs and Ag^+ in CHO-K1 cells is proposed.

2. Materials and methods

2.1. Materials and reagents

Ham's F-12K (Kaighn's) medium, heat-inactivated foetal bovine serum (FBS), L-alanyl-L-glutamine, penicillin and streptomycin, Annexin V-Alexa488, propidium iodide (PI), ethidium monoazide bromide (EMA) and SYTOX Green were purchased from Invitrogen. 2′,7′-Dichlorodihydrofluorescein diacetate (H_2DCF-DA), 7-aminoactinomycinD (7-AAD), 3-(4,5-dimethyl-2-thiazolyl)-2,5-diphenyl-2H-tetrazolium bromide (MTT), dimethylsulfoxide (DMSO), RNase, HEPES, NaCl, $CaCl_2$, $AgNO_3$ (Reagent Part of the European Pharmacopoeia), sodium citrate tribasic dehydrate, sodium borohydride ($NaBH_4$), bovine serum albumin (BSA) and phosphate-buffered saline (PBS) were purchased from Sigma–Aldrich. Nuclear Isolation and Stain solution containing 4′,6-diamidino-2-phenylindole (NIM-DAPI) was purchased from Beckman Coulter.

2.2. Cell culture

The Chinese Hamster Ovary cells – subclone K1 (CHO-K1) cell line was obtained from German Collection of Microorganisms and Cell Cultures (DSMZ, ACC-110). Cells were cultured in F-12K medium supplemented with 5% heat-inactivated foetal bovine serum (FBS) and penicillin (100 μg/ml), streptomycin (100 U/ml) (hereafter referred to as cell culture medium) and maintained at 37 °C in a humidified atmosphere of 5% CO_2.

For all experiments cells were seeded in culture dishes or flasks one day prior to the exposure in the cell culture medium. For the exposure studies, Ag NP stock suspension (or water for controls) was diluted in the cell culture medium. The silver concentration applied in the study refers to the mass concentration of silver atoms.

2.3. Transmission electron microscopy of fixed cells

Intracellular localization of Ag NPs in CHO-K1 cells was studied by TEM. Cells were seeded in 24-well plates and grown until 90% confluency. After 24 h exposure to Ag NPs, cells were washed with PBS and subsequently fixed with glutaraldehyde (2%). Finally, cells were imbedded, cut into ultrathin slices, and observed under TEM.

2.4. Inductively coupled plasma mass spectrometry analysis

To study the cellular uptake of Ag NPs, inductively coupled plasma mass spectrometry analysis (ICP-MS, Thermo Elemental X7, Thermo Fisher Scientific Inc., USA) was conducted. Briefly, cells were exposed to Ag NPs or Ag^+ in a concentration series for 24 h. After incubation, cells were washed three times with PBS, collected, and small aliquots of each cell suspension were stained with trypan-blue and examined using an automated cell counter (Countess, Invitrogen). The cell pellet was soaked in aqua regia overnight and heated to about 140 °C to vaporize hydrogen chloride and nitrogen oxides until the solution became clear. After adding up to 3 ml using solvent matrix containing 2% nitric acid and 1% hydrogen chloride, silver content was analyzed using ICP-MS. Bismuth of 10 ng/ml was used as an internal standard. The concentration of elemental silver in the solution was thus obtained.

2.5. MTT assay

Mitochondrial activity of CHO-K1 cells was analyzed using the MTT assay as previously described (Mosmann, 1983) with minor modifications. Briefly, cells were seeded in 96-well plates with 8×10^3 cells per well and allowed to attach overnight. After 24 h exposure to Ag NPs or Ag^+, the cells were washed with PBS and incubated with MTT (0.5 mg/ml, dissolved in the cell culture medium without FBS) for 2 h at 37 °C. The MTT solution was discarded and DMSO (100 μl/well) was added, and the plate was rigorously shaken for 2 min to dissolve the dye. The optical density was read on a microplate reader at 570 nm, with a reference at 655 nm (EL800, Bio-Tek Instruments, Inc.). The mitochondrial activity of Ag NPs or Ag^+-treated cells was normalized to that of the negative controls.

2.6. Reactive oxygen species

Intracellular reactive oxygen species (ROS) was measured by the oxidation-sensitive fluoroprobe 2′,7′-dichlorodihydrofluorecein diacetate (H_2DCF-DA, Invitrogen) as described previously (Hayashi et al., 2012; Lao et al., 2009b) with minor modifications. The cell-permeable, non-fluorescent H_2DCF-DA compound is converted to the highly fluorescent 2′,7′-dichlorofluorescein (DCF) by intracellular oxidants, indicating the level of intracellular ROS. In brief, cells were seeded in 6-well plates with 5×10^4 cells per well and exposed to a concentration series of Ag NPs or Ag^+ for 24 h. Subsequently, the cells were washed once with PBS and the fluorescent marker H_2DCF-DA (5 μg/ml) was added to each well and incubated at 37 °C for 30 min. The cells were washed with PBS, harvested and resuspended in 500 μl PBS containing the DNA stain, 7-AAD (1 μg/ml), and analyzed by flow cytometry (Cell Lab Quanta SCMPL, Beckman Coulter). The 488 nm laser was used for excitation and fluorescence was detected in FL-1 with a 525/30 BP filter and FL-3 with a 670 LP filter. Control experiments showed that Ag NPs or Ag^+ does not interfere with H_2DCFDA and the ROS assay (data not shown). For each sample, the mean fluorescence of 2×10^4 viable cells (7-AAD negative) was determined.

2.6.1. Cell cycle analysis

Cell cycle analysis was performed using NIM-DAPI and subsequent flow cytometry analysis as described previously (Foldbjerg et al., 2012).

2.6.2. Apoptosis and necrosis assay

The ratio of apoptotic and necrotic cells were measured with the annexin V/propidium iodide (PI) assay (Van Engeland et al., 1996).

As a marker of early-stage apoptosis, the externalization of phosphatidylserine was measured by binding of Alexa 488-conjugated annexin V protein to phosphatidylserine. Late-stage apoptosis and necrosis was detected by the binding of PI to nuclear DNA due to cellular membrane damage. Annexin V/PI assay was performed as described previously (Foldbjerg et al., 2011) with minor modifications. In brief, CHO-K1 cells were seeded in 6-well plates with 2×10^5 cells per well. After exposure to different concentrations of Ag NPs or Ag^+ for 24 h, cells were washed with PBS and trypsinized, centrifuged and resuspended in 100 μl binding buffer (10 mM HEPES, pH 7.4; 140 mM NaCl; 2.5 mM $CaCl_2$) containing Annexin V-Alexa488 (40 μl/ml) and PI (1 μg/ml). The samples were incubated for 10 min at RT, protected from light. Subsequently, 400 μl binding buffer was added to each sample and cells were kept on ice until analysis. A 488 nm wavelength laser was used for excitation. Alexa-488 was detected in FL-1 using a 525/30 BP filter while PI was detected in FL-2 using a 575/30 BP filter. Using single-stained and unstained cells, standard compensation was done in the Quanta SC MPL Analysis software (Beckman Coulter). For each sample, 2×10^4 cells were analyzed and early apoptotic (annexin V+, PI−), late apoptotic/necrotic (annexin V+, PI+) and live (annexin V−, PI−) cells were expressed as percentages of the measured 2×10^4 cells using the FlowJo software ver. 7.6.4 (Tree Star, Inc.).

2.7. Bulky DNA adduct analysis

DNA adducts were determined by the ^{32}P-Postlabeling method, which is a sensitive method to detect DNA damage induced by carcinogens. Briefly, cells were seeded in 6 cm plates and grown until 90% confluence. After Ag NP and Ag^+ exposure for 24 h, cells were lysed and DNA was isolated. DNA adducts were determined by the butanol enrichment procedure as previously described (Bak et al., 2005; Nielsen et al., 1996). The adduct spots were measured by phosphorimage analysis (Molecular Image, Bio-Rad GS-363). The BaP-diolepoxide DNA adduct was included in the analysis as an internal standard. The level of DNA adducts was obtained as the average of three independent assays and expressed as adducts per 10^8 nucleotides ($n/10^8$ nucleotides). The detection limit was 0.1 $n/10^8$ nucleotides.

2.8. 8-oxodG analysis

8-oxo-2′-deoxyguanosine (8-oxodG) in DNA was measured using positive electrospray ionization online column-switching liquid chromatography/tandem mass spectrometry (LC/MS/MS) as described earlier (Singh et al., 2009). Briefly, cells were seeded in 75 cm^2 cell culture flask and exposed to Ag NPs or Ag^+ for 24 h. After exposure, cells were collected and DNA was isolated. The isolated DNA was enzymatically hydrolyzed and analyzed by LC/MS/MS. To allow for the accurate quantitation of adducts the corresponding [^{15}N5]-labelled stable isotope internal standards were synthesized and added prior to enzymatic hydrolysis of the DNA samples to 2-deoxynucleosides. The detection limit was 5 fmol.

2.8.1. Fluorescence microscopy-based micronucleus assay

Micronucleus assay with fluorescence microscope was performed as described by Fenech (2007) with minor modifications. Briefly, cells were seeded on coverslips in a 24-well plate with 2×10^4 cells per well. The cells were treated with different concentrations of Ag NPs or Ag^+ for 24 h exposure. Cells were washed once with PBS and 6 μg/ml cytochalasin B in a fresh cell culture medium was added for 36–48 h to block the cell cycle. Subsequently, the cells were washed with PBS and fixed with 1% paraformaldehyde for 15 min at RT. The coverslips were washed with PBS and placed on a drop of mounting medium containing DAPI (VectaShield) on an objective slide and observed by fluorescence microscopy (Leica) using a DAPI filter.

2.9. Flow cytometry-based micronucleus assay

Flow cytometry based micronucleus assay was conducted using the *in vitro* MicroFlow micronucleus analysis kit (LitronLabs) following manufacturer's instruction. In brief, cells were seeded in 12-well plates with 2×10^4 cells per well. Different concentrations of Ag NPs or Ag^+ were added for 24 h exposure. Subsequently, the cells were incubated in a new cell culture medium at 37 °C for 24 h to allow for 1 or 2 cell cycles. Subsequently, a nuclear fluorescent dye ethidium monoazide bromide (EMA) was added to stain the cells with damaged membrane. After washed with PBS (contain 2% FBS), cells were lyzed and stained with SYTOX Green, and collected for flow cytometry analysis. Nuclei with SYTOX positive and EMA negative staining and smaller sized particles were recorded as micronuclei. For each sample, 5×10^4 total events were collected and analyzed as described by the manufacturer and Bryce et al. (2007) using a 3 Laser FACS Aria III (BD Biosciences).

2.10. Statistical analysis

Data are expressed as mean ± standard deviation (SD) of three independent experiments. The statistical significance was determined by the Student's *t*-test ($p < 0.05$).

3. Results

3.1. Cellular uptake and intracellular localization of Ag NPs

BSA coated Ag NPs (mean particle size = 15.9 ± 7.6 nm, $n = 490$) were used in this study (the characterization data can be found in ref (Foldbjerg et al., 2012)). To show that CHO-K1 cells are able to take up these Ag NPs, the cells were exposed to Ag NPs for 24 h and transmission electron microscopy (TEM) was employed to observe the intracellular localization of Ag NPs (Fig. 1). The TEM analysis suggests that Ag NPs can be found in endosomes or lysosomes, however, in the samples we analyzed no Ag NPs were found in mitochondria or the nucleus.

In order to quantify the Ag NPs that have been taken up by the cells, inductively coupled plasma mass spectrometry (ICP-MS) was applied. The concentration of silver atoms in acid digesting solution was directly measured and the concentration of silver per 10^4 cells was calculated according to the number of cells in the sample before digestion. As shown in Fig. 2, there is a concentration-dependent increase of Ag per 10^4 cells.

3.2. Mitochondrial activity and production of reactive oxygen species (ROS)

The mitochondrion is the energy factory of cells, which plays a significant role in cell growth and proliferation. As a measure for cell viability, the mitochondrial activity of CHO-K1 cells after exposure to Ag NP and Ag^+ for 24 h was determined using the MTT assay. In order to ensure that Ag NPs do not interfere with the MTT assay, we used cell free medium with different concentrations of Ag NPs as a control and showed that Ag NPs do not interfere with the MTT reagent and the optical measurements (data not shown). As is shown in Fig. 3(A), mitochondrial activity decreased in a concentration-dependent manner following both Ag NP and Ag^+ exposure. The IC_{50} (half inhibition concentration) of Ag NPs and Ag^+ were 15 and 10 μg/ml, respectively. Interestingly, there is only a statistical significant difference of the cell viability of Ag NP and Ag^+ treated cells at 20 μg/ml where Ag^+ inhibited the cell viability

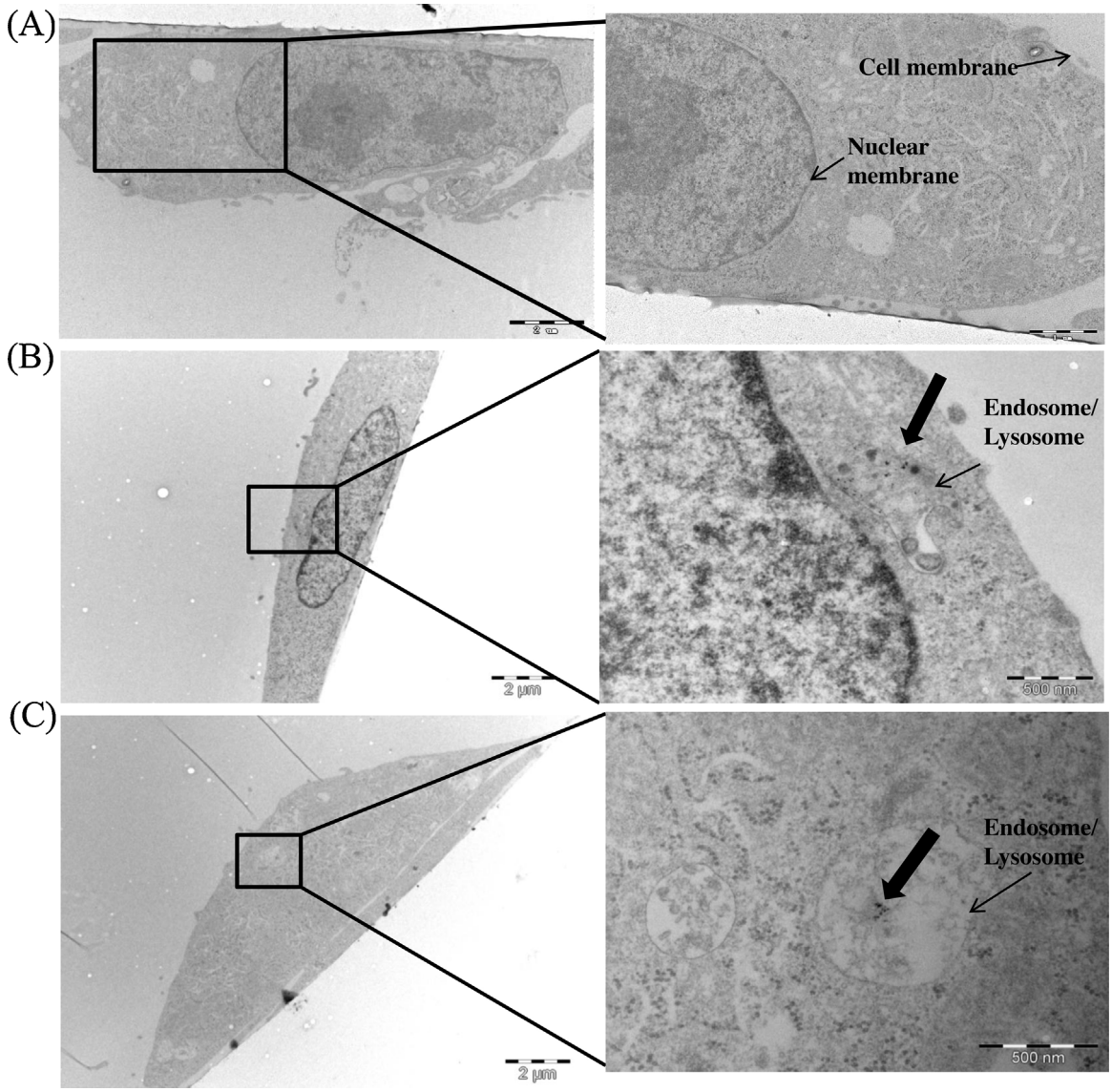

Fig. 1. TEM images of CHO-K1 cells. CHO-K1 cells without Ag NPs exposure (A). CHO-K1 cells treated with 10 μg/ml Ag NPs for 6 h (B) and 24 h (C). Broad arrows indicate Ag NPs. Narrow arrows indicate cell membrane and nuclear membrane. Ag NPs were visible in endosomes/lysosomes indicating a receptor mediated endocytosis. No Ag NPs were observed in mitochondria or nuclei. The scale bar for the left panel is 2 μm, 1 μm for the top one of the right panel and 500 nm for the rest.

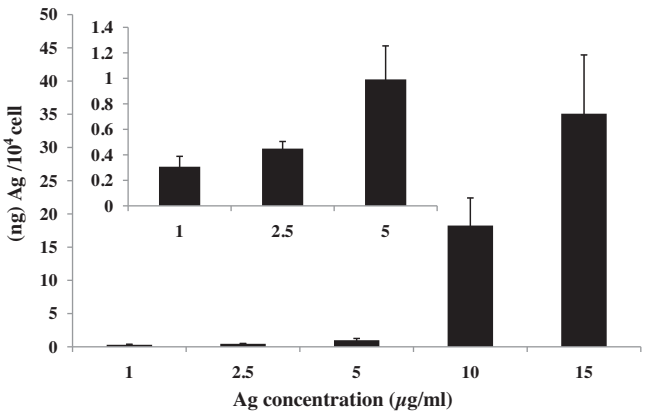

Fig. 2. Concentration-dependent cellular uptake of Ag NPs in CHO-K1 cells after 24 h exposure to 1–15 μg/ml Ag NPs. The Ag concentration was measured using ICP-MS and calculated by dividing by cell number and expressed as ng Ag per 10^4 cells. The data are expressed as mean ± SD of three independent experiments.

by more than 90% while Ag NPs only inhibited the cell viability by 60%.

Oxidative stress has been considered the common way for nanomaterial-induced toxicity (Foldbjerg et al., 2011; Kim et al., 2009). ROS are essential in signal transduction for cell growth and proliferation. But high levels of ROS induce various dysfunctions of cells including membrane damage, DNA and protein damage, apoptosis or necrosis (Hsin et al., 2008; Kim et al., 2011; Wang et al., 2010). A ROS assay combined with 7-AAD staining of dead cells was applied to evaluate the ROS level in live cells. As is shown in Fig. 3(B), the ROS level increased in a concentration-dependent manner upon Ag NPs and Ag^+ exposure. In accordance with the cell viability data of the MTT assay, Ag^+ induced an approximately 2-fold increase in ROS compared to the control, whereas Ag NPs increased the ROS level only to about 1.8-fold, at a silver concentration of 10 μg/ml. However, although Ag^+ induced higher ROS levels at all measured concentrations these differences were not statistically significant. Control experiments showed that Ag NPs or Ag^+ does not interfere with H_2DCFDA and the ROS assay (data not shown).

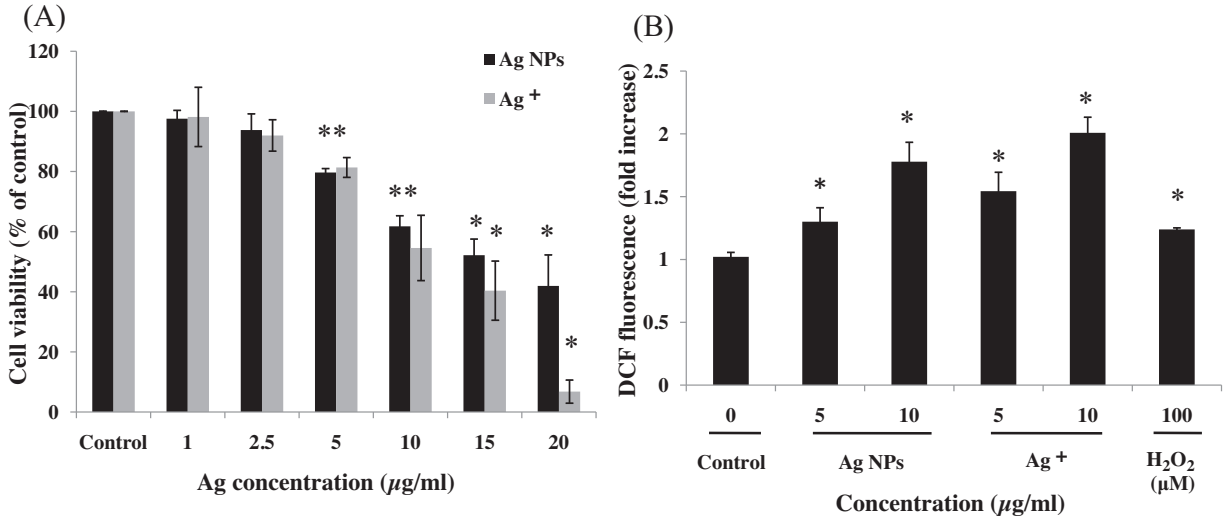

Fig. 3. Mitochondrial activity and intracellular ROS level of cells exposed to Ag NPs and Ag^+ for 24 h. (A) The change in the mitochondrial activity of CHO-K1 cells after exposure to different concentrations of Ag NPs and Ag^+ for 24 h. (B) The change in intracellular ROS levels in CHO-K1 cells after exposure to different concentration of Ag NPs or Ag^+ for 24 h. H_2O_2 (100 μM) was employed as a positive control. The samples were normalized relative to the negative control. The data are expressed as mean ± SD of three independent experiments. Statistically significant difference from controls are expressed as *($p < 0.05$).

3.3. Cell cycle and induction of apoptosis and necrosis

We have previously demonstrated that exposure of cells to Ag NPs results in cell cycle arrest and induction of apoptosis in human cell lines (Foldbjerg et al., 2011, 2012). Considering that genotoxicity assays like the micronucleus assay require cell division, we investigated the effect of Ag NPs and Ag^+ on the cell cycle of CHO-K1 cells. Our results indicate that at concentrations lower than 10 μg/ml, Ag NPs do not significantly affect the cell cycle (Fig. 4A and B). Although not statistically significant, at 10 μg/ml, a slight increase of cells in the G2/M phase and decrease of cells in the G1 phase were observed. At higher concentrations this effect was even more pronounced (data not shown). In addition, Ag^+ induced a concentration-dependent increase in subG1, which indicates fragmentation of the nucleus due to cell death. In Ag NP-treated cells, only a minor increase in subG1 at 10 μg/ml was observed. The presence of cells in subG1 phase is in agreement with results from the Annexin V/PI assay that examines apoptosis and necrosis. As shown in Fig. 4C and D, Ag NPs and Ag^+ induced an increase in early apoptotic cells at 10 μg/ml. At the concentration of 10 μg/ml silver, Ag^+ induced a statistically significant slight increase in late apoptotic/necrotic cells, whereas this was not the case for Ag NPs. Taken together, Ag^+ is more cytotoxic to CHO-K1 cells than Ag NPs at the same concentration of silver.

3.4. Bulky DNA adducts and 8-oxodG

We have shown that exposure of cells to Ag NPs and Ag^+ leads to an increased level of intracellular ROS, a known inducer of DNA damage. Therefore, ^{32}P-Postlabelling was applied to measure bulky DNA adduct levels. Both Ag NPs and Ag^+ increased the amount of DNA adducts in a concentration-dependent manner (Fig. 5). However, when comparing identical Ag concentrations, Ag^+ induced approximately 2-fold more bulky DNA adducts than Ag NPs (Fig. 5).

8-oxodG, a marker for oxidative DNA damage, was determined by LC/MS/MS. At 10 μg/ml of silver, Ag NPs and Ag^+ induced an increase in the 8-oxodG level, indicating oxidative DNA damage (Fig. 6). Noticeably, the amount of 8-oxodG increased after Ag NP exposure by approximately 2-fold in a concentration-dependent manner compared to only a 1.3-fold increase for Ag^+ at 10 μg/ml total silver. This suggests that there is a quantitative and qualitative difference in how DNA damage is induced by Ag^+ and Ag NPs.

3.5. Fluorescence microscope and flow cytometry based micronucleus assay

To further analyze the genotoxic potential of Ag NPs and Ag^+, fluorescence microscopy and a flow cytometry-based micronucleus assays were performed. As shown in Fig. 7, untreated control cells were blocked in the anaphase, nearly all of the cells were binucleated and micronuclei were only occasionally observed. In the Ag NPs and Ag^+ exposure groups, micronuclei were more frequently observed in the binucleated cells. In addition, we noticed several enlarged nuclei and at higher silver concentrations the number of binucleated cells decreased suggesting a cell cycle arrest. As the quantification of micronuclei by fluorescence microscopy is time consuming, we used a flow-cytometric micronucleus assay developed by Bryce et al. (2007) to quantify the increase in micronucleus formation. As shown in Fig. 8, both Ag NPs and Ag^+ induced a concentration-dependent formation of micronuclei. However, at 10 μg/ml of silver, Ag^+ induced 1.7-fold more micronuclei than Ag NPs.

4. Discussion

Toxicity of Ag NPs and their potential adverse health effects have been raising more and more concerns due to their widespread application in commercial products, such as household and healthcare products, food package, and clothes (Busolo et al., 2010; Chen et al., 2006; Samuel and Guggenbichler, 2004). Many articles regarding the cytotoxicity and genotoxicity of Ag NPs have been published during recent years (AshaRani et al., 2008; Foldbjerg et al., 2009, 2011). However, studies regarding Ag NPs induced DNA adducts, especially oxidative DNA damage product 8-oxodG in Chinese hamster ovary (CHO-K1) cells are rare. Here, we compared Ag NPs with Ag^+ and systemically investigated their genotoxic and cytotoxic effects on CHO-K1cells, a cell line, which is recommended by the OECD for the standardized quantification of micronuclei formation (OECD guideline #487).

Regarding the interactions between nanomaterials and cells, the cellular uptake and subsequent toxic response of the cell are one

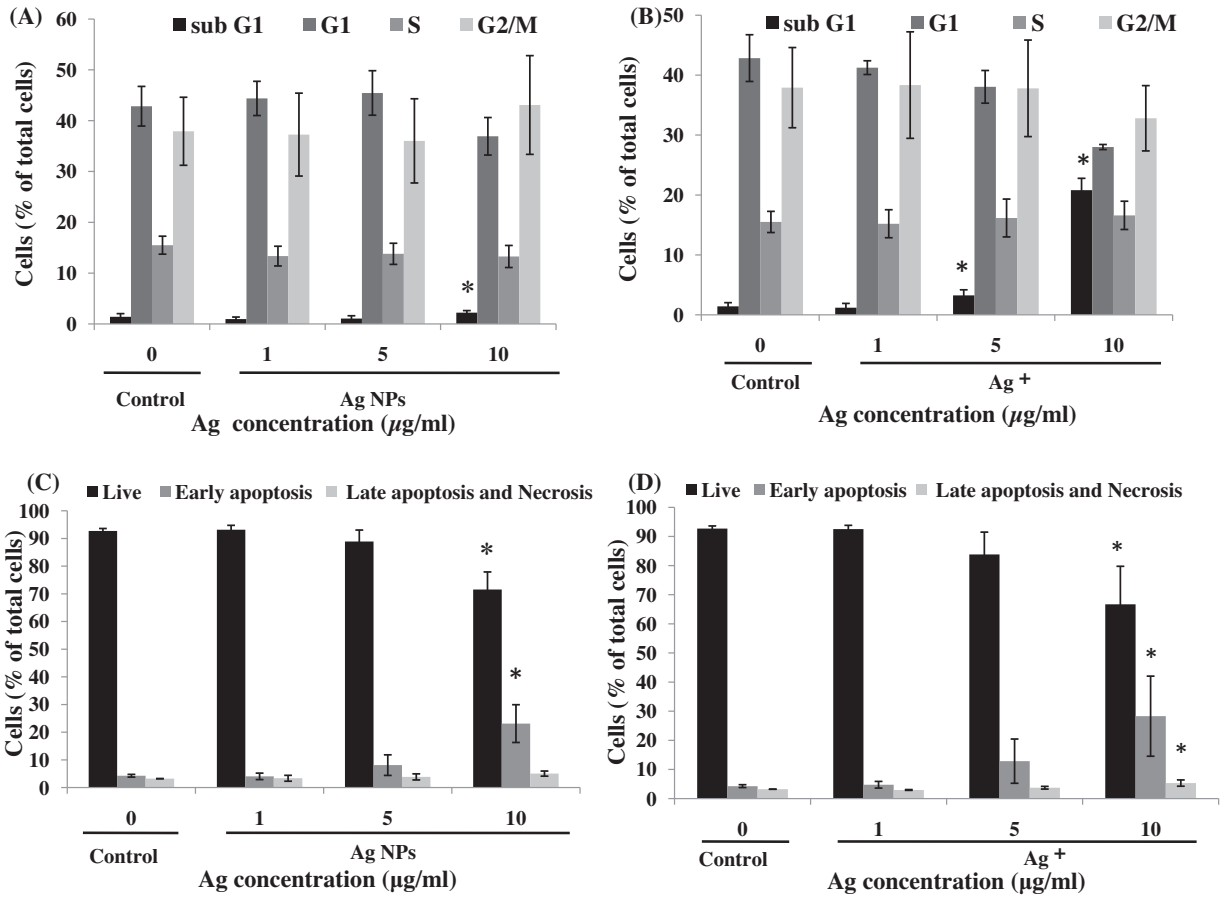

Fig. 4. Cell cycle, apoptosis and necrosis in cells after 24 h exposure to Ag NPs or Ag^+. The changes in cell cycle were measured after 24 h exposure to (A) Ag NPs and (B) Ag^+. The annexin V/PI assay was used to assess the percentage of viable, apoptotic and necrotic cell fractions induced by 24 h treatment with (C) Ag NPs and (D) Ag^+. Negative control cells were cultured in NP-free media. The data are expressed as mean ± SD of three independent experiments. Statistically significant difference from control is expressed as *($p < 0.05$).

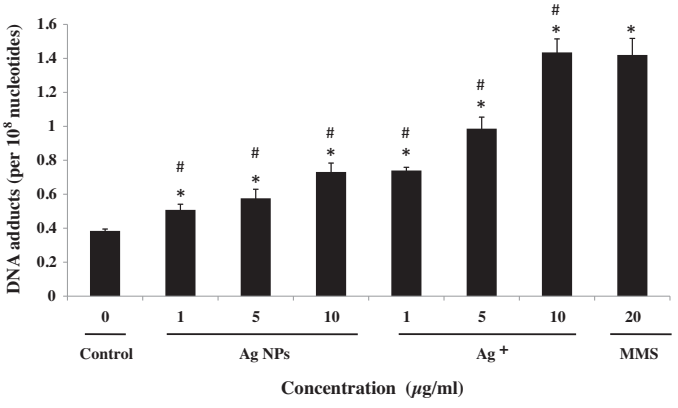

Fig. 5. DNA adducts induced by Ag NPs and Ag^+ exposure for 24 h. After exposure to different concentrations of Ag NPs and Ag^+, cells were collected and the DNA was isolated and analyzed by the ^{32}P-Postlabeling method. The data are expressed as mean ± SD of three independent experiments. Statistically significant difference from control is expressed as * ($p < 0.05$) and significant difference between Ag NPs and Ag^+ in the same amount of silver is expresses as # ($p < 0.05$).

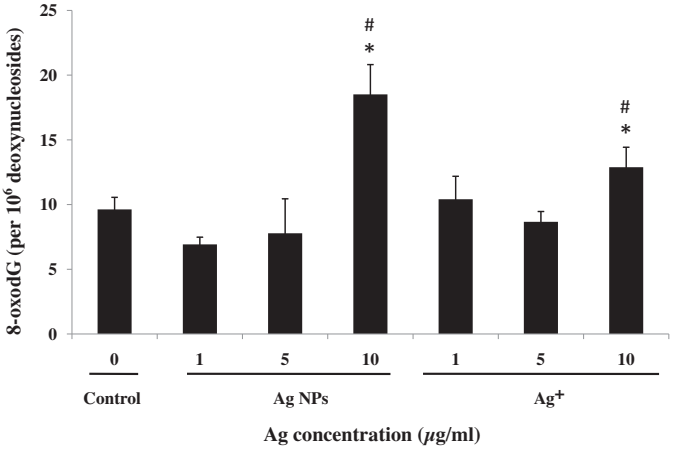

Fig. 6. 8-oxodG induced by Ag NPs and Ag^+ exposure for 24 h. After exposure to different concentrations of Ag NPs and Ag^+, cells were collected and the DNA was isolated and analyzed by LC/MS/MS. The data are expressed as mean ± SD of three independent experiments. Statistically significant difference from control is expressed as * ($p < 0.05$) and significant difference between Ag NPs and Ag^+ in the same amount of silver is expresses as # ($p < 0.05$).

of the most critical issues. Due to their nanoscale size in all three dimensions (between 1 and 100 nm), nanoparticles are easily taken up by cells through, *e.g.*, endocytosis, and transferred to different organelles (Chithrani et al., 2009; Lao et al., 2009a; Porter et al., 2006). Flow cytometry has been suggested a robust technique to measure the cellular accumulation of Ag NPs in correlation to the increase in the side scatter of the cell (Toduka et al., 2012). However, it is not possible to quantify the uptake by this technique. Therefore, we quantified the cellular accumulation of Ag NPs using ICP-MS. The results demonstrated a concentration-dependent cellular accumulation of Ag NPs following 24 h exposure. However, it

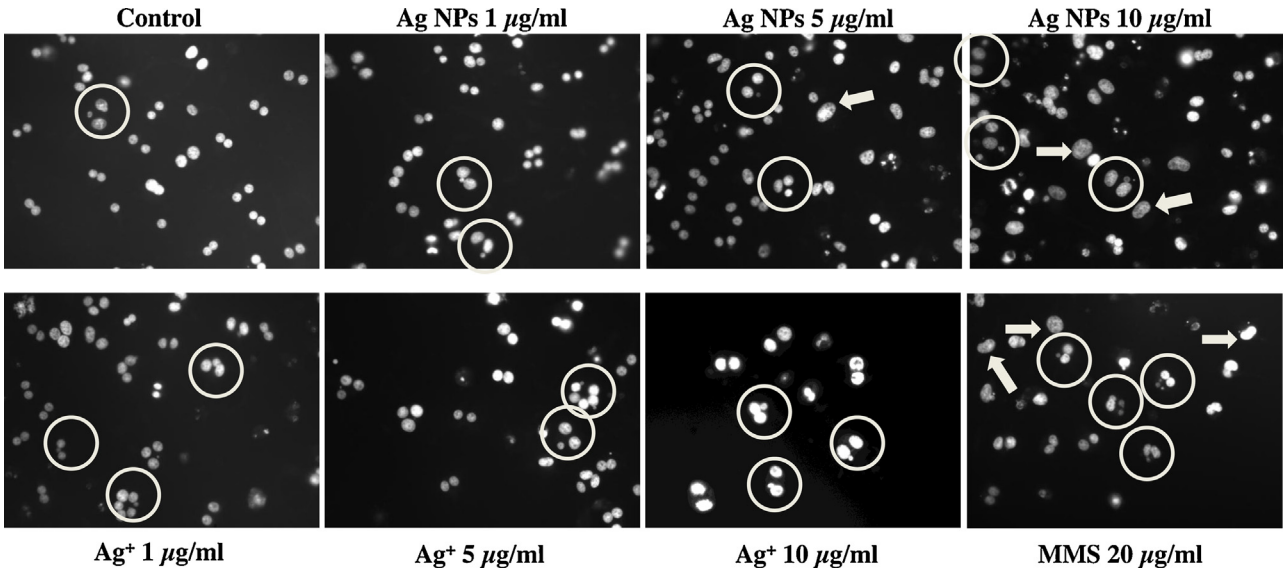

Fig. 7. Fluorescence microscopy images of micronuclei induced by Ag NPs and Ag^+ exposure for 24 h. Cell cycle was blocked by cytochalasin B. Nuclei were stained with DAPI. Methyl methanesulphonate (MMS) was employed as positive control. Micronuclei in the binucleated cells are indicated with circles. Cells blocked in G2/M phase were indicated with filled arrows.

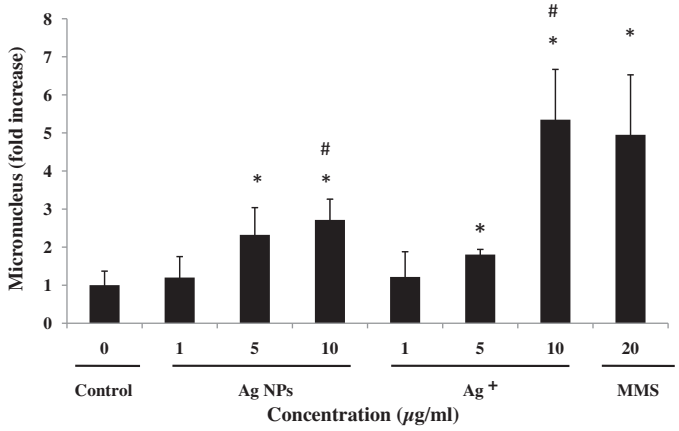

Fig. 8. Flow cytometry analysis of micronuclei formation induced by Ag NPs and Ag^+ exposure for 24 h. The data are expressed as mean ± SD of at least three independent experiments. Statistically significant difference from control is expressed as * ($p < 0.05$) and significant difference between Ag NPs and Ag^+ in the same amount of silver is expresses as # ($p < 0.05$).

should be noted that even though the cells were washed three times and trypsinized after Ag NPs exposure, it is likely that not all Ag NPs were removed from the cell surface. Therefore, the amount of silver per cell measured from the ICP-MS analysis reflects a combination of Ag NPs inside and on the cells. The same is true for measuring the uptake of Ag NPs by flow cytometry and to our knowledge, to date, there does not exist a quantification technique which is truly able to differentiate extracellular from intracellular Ag NPs.

Intracellular localization plays an important role in nanomaterial-induced toxicity. Recent studies reported that endosomes and lysosomes are the most common compartments for nanomaterial localization (Chithrani and Chan, 2007; Peckys and de Jonge, 2011). Some nanomaterials localize in mitochondria and the nucleus (Hackenberg et al., 2011; Raoof et al., 2012). As mitochondria and the nucleus are important functional compartments of cells playing significant roles in cell metabolism and proliferation, localization of nanomaterials in mitochondria and in the nucleus may induce sever interference in cellular functions. Studies with gold nanomaterials showed that they did not induce significant cytotoxicity with no evidence of them entering mitochondria or the nucleus (Wang et al., 2010). Previous studies showed that Ag NPs could enter mitochondria and the nucleus (AshaRani et al., 2008). In contrast, localization of Ag NPs not in the nucleus but in endoplasmic reticulum and mitochondrion has also been reported (Wei et al., 2010). Our study suggests that Ag NPs are located in endosomes and/or lysosomes, whereas no Ag NPs were found in mitochondria or the nucleus. But unlike gold nanomaterials, endocytosed Ag NPs may liberate Ag^+ and can thereby induce cell-specific, localized cellular toxicity as suggested by the Trojan horse theory (Park et al., 2010).

Mitochondria are of critical importance for the energy production of cells. Here, we showed a concentration-dependent decrease in the mitochondrial activity following 24 h Ag NPs or Ag^+ exposure, which is consistent with the observed concentration-dependent cellular uptake. The IC_{50} for Ag NPs and Ag^+ are 15 and 10 μg/ml, respectively, which suggests that Ag^+ are more toxic than Ag NPs. It is worth to mention that the water-soluble tetrazolium salt 8 (WST-8 or the cell counting kit CCK-8) assay, an alternative to MTT assays, is not appropriate for the cytotoxicity evaluation of Ag NPs that exhibit surface plasmon resonance peak around 400–500 nm in wavelength. Our results (data not shown) demonstrated that the absorption of the end products (WST-8 formazan dye), when measured at 450 nm, was interfered by the presence of Ag NPs leading to false positive results. Therefore, choosing the appropriate assay is of vital importance when evaluating the cytotoxicity of nanomaterials.

ROS induction has been suggested as a common pathway for nanomaterial-induced toxicity. In this study we showed that both Ag NPs and Ag^+ increased the intracellular ROS level. However, although not statistically significant, Ag^+ induced more ROS than Ag NPs at the same silver concentration. Increased ROS level is related to a series of events leading to, *e.g.*, membrane damage, DNA and protein damage, apoptosis or necrosis (Hsin et al., 2008; Kim et al., 2011; Wang et al., 2010). In addition, DNA damage leads to an arrest in the cell cycle to allow repair enzymes to correct DNA damages (Ishikawa et al., 2006). Therefore, several cell cycle check points exist, including checkpoint G_0/G_1, G_1/S, G_2/M. Our studies suggest an Ag NP-induced arrest in G2/M for CHO-K1 cells exposed to Ag NP but also an increase in subG1 phase, which is a sign of DNA fragmentation. In addition, the arrest in cell cycle is consistent with our observation from the fluorescence microscopy-based

micronucleus assay that Ag NPs exposure resulted in abnormally large nuclei instead of binucleated cells when cells were treated with cytochalasin B. This suggests that the cells were arrested in the cell cycle and failed to undergo cell division (Fig. 7). If the DNA is damaged beyond repair, the cellular machinery initiates programmed cell death or apoptosis. Accordingly, the Annexin V/PI assay and the increase in subG1 phase showed that both Ag NPs and Ag^+ induced an increase in apoptotic cells. These results indicated that exposure to Ag NPs or Ag^+ may induce DNA damage, which was confirmed by ^{32}P-Postlabeling of bulky DNA adducts, quantitation of 8-oxodG and micronucleus formation, respectively. It is generally believed that the formation of DNA adducts is an essential first step in the multistage process of carcinogensis. Oxidative DNA damage marker-8-oxodG has been studied both *in vivo* and *in vitro* (Chen et al., 2005; Dwivedi et al., 2012). Other studies showed that, the formation of 8-oxodG can lead to chromosomal aberrations and the induction of mutations, which mainly involve GC to TA transversions. We have previously reported that Ag NPs induced bulky DNA adducts in A549 cells, and that the adduct formation was inhibited by antioxidants (Foldbjerg et al., 2011). An epidemiological study reported bulky DNA adducts are associated with an increased risk of cancer (Bak et al., 2005). ROS has been considered the major source of spontaneous damage to DNA (Foldbjerg et al., 2011; Kim et al., 2011). The chemical reactions that result in such mutations are based on the formation of highly reactive and short-lived hydroxyl radicals ($OH^•$) in close proximity to DNA (Cadet et al., 1999). ROS-mediated genotoxicity has previously been observed for metal oxide nanoparticles (Yang et al., 2008). Here, we measured the specific DNA oxidative adduct 8-oxo-7,8-dihydro-2′-deoxyguanosine (8-oxodG), which is formed by the hydroxylation of the C-8 position of guanine (Kasai, 1997). Furthermore, chromosome abnormalities are a direct consequence of DNA damages such as double strand breaks and misrepair of strand breaks, resulting in chromosome rearrangement. Micronuclei (MN) are formed in dividing cells from chromosome fragments or whole chromosomes that were unable to engage with the mitotic spindle during mitosis (Fenech, 2006). Here, we demonstrated that both Ag NPs and Ag^+ exposure increased the amount of bulky DNA adducts and the 8-oxodG levels as well as the micronucleus formation in CHO-K1cells in a concentration-dependent manner. However, it is important to notice that there are differences in the genotoxicity of Ag NPs and Ag^+. While Ag^+ induced the formation of bulky DNA adducts and micronuclei approximately 2-fold more than Ag NPs, the amount of 8-oxodG was 44% higher in cells exposed to Ag NPs compared to cells exposed to Ag^+.

In summary, both exposure to Ag NPs and Ag^+ induced cyto- and genotoxicity but Ag^+ appeared to be more (geno)-toxic at the same silver concentration than Ag NPs in CHO-K1 and our results suggest mechanistically differences of the genotoxic mode of action for Ag NPs and Ag^+. These results indicate that applications of Ag NPs in commercial products need to be carefully evaluated. In this context, we speculate that specific surface modifications inhibiting Ag^+-release may reduce the toxicity of Ag NPs.

5. Conclusions

Investigating the DNA damaging effects of chemicals is done by, *e.g.*, studying the formation of micronuclei. According to the OECD guidelines the Chinese hamster ovary cell line CHO-K1 is one of the recommended cell lines for the standardized investigation of micronucleus formation (OECD Guidelines for the Testing of Chemicals Test No. 487: *In Vitro* Mammalian Cell Micronucleus Test). However, CHO-K1 cells are rarely used for genotoxicity studies on nanoparticles. Here, we systematically investigated the cytotoxicity of Ag NPs in relation to their DNA damaging properties like the formation of micronuclei and DNA adducts, especially oxidative DNA damage products like 8-oxodG in comparison to Ag^+. We demonstrated that silver, both as nanoparticles and in ionic form, induced DNA adducts, 8-oxodG and micronuclei formation in CHO-K1 cells in a concentration-dependent manner. Cytotoxicity studies showed decreased mitochondrial activity, increased intracellular ROS, and apoptosis and necrosis. All the observed toxic effects induced by Ag NPs were also induced by Ag^+ and demonstrates that CHO-K1 cells are suitable for the investigation of genotoxicity of nanoparticles like Ag NPs. Except from the formation of 8-oxodG, Ag^+ generally appeared as more toxic and suggest quantitative and qualitative differences of the mode of action between the particulate and ionic form of silver. Based on the quantity of elemental silver per cell as measured by ICP-MS in combination with the cytotoxicity and genotoxicity data, we suggest that Ag NPs were dissolved into Ag^+ and that the cytotoxicity and genotoxicity mostly resulted from the bioactive Ag^+ released from Ag NPs. The released Ag^+ possibly enter mitochondria and the nucleus, causing the increased intracellular ROS levels as well as DNA and chromosomal damage. However, further studies on Ag^+ release from Ag NPs inside cells should be performed to support this hypothesis.

Conflict of interest declaration

The authors declare that there are no conflicts of interest.

Acknowledgements

The authors thank Duy Anh Dang for the assistance with bulky DNA adducts analysis, Karen Thomsen for her assistance with TEM, Charlotte Christie Petersen and Anette Thomsen for their assistance with flow cytometry-based micronucleus assay. This work was supported by the Danish Council for Strategic Research grant (09-067185) and the Ministry of Science and Technology of China (2011CB933401).

References

Ahamed, M., Karns, M., Goodson, M., Rowe, J., Hussain, S.M., Schlager, J.J., Hong, Y., 2008. DNA damage response to different surface chemistry of silver nanoparticles in mammalian cells. Toxicology and Applied Pharmacology 233, 404–410.

AshaRani, P., Low Kah Mun, G., Hande, M.P., Valiyaveettil, S., 2008. Cytotoxicity and genotoxicity of silver nanoparticles in human cells. ACS Nano 3, 279–290.

Bak, H., Autrup, H., Thomsen, B.L., Tjønneland, A., Overvad, K., Vogel, U., Raaschou-Nielsen, O., Loft, S., 2005. Bulky DNA adducts as risk indicator of lung cancer in a Danish case-cohort study. International Journal of Cancer 118, 1618–1622.

Beer, C., Foldbjerg, R., Hayashi, Y., Sutherland, D.S., Autrup, H., 2011. Toxicity of silver nanoparticles–nanoparticle or silver ion? Toxicology Letters 208, 286–292.

Bryce, S.M., Bemis, J.C., Avlasevich, S.L., Dertinger, S.D., 2007. In vitro micronucleus assay scored by flow cytometry provides a comprehensive evaluation of cytogenetic damage and cytotoxicity. Mutation Research – Genetic Toxicology and Environmental Mutagenesis 630, 78–91.

Busolo, M.A., Fernandez, P., Ocio, M.J., Lagaron, J.M., 2010. Novel silver-based nanoclay as an antimicrobial in polylactic acid food packaging coatings. Food Additives and Contaminants A 27, 1617–1626.

Cadet, J., Delatour, T., Douki, T., Gasparutto, D., Pouget, J.P., Ravanat, J.L., Sauvaigo, S., 1999. Hydroxyl radicals and DNA base damage. Mutation Research – Fundamental and Molecular Mechanisms of Mutagenesis 424, 9–21.

Chairuangkitti, P., Lawanprasert, S., Roytrakul, S., Aueviriyavit, S., Phummiratch, D., Kulthong, K., Chanvorachote, P., Maniratanachote, R., 2012. Silver nanoparticles induce toxicity in A549 cells via ROS-dependent and ROS-independent pathways. Toxicology in Vitro 27, 330–338.

Chen, C., Qu, L., Li, B., Xing, L., Jia, G., Wang, T., Gao, Y., Zhang, P., Li, M., Chen, W., 2005. Increased oxidative DNA damage, as assessed by urinary 8-hydroxy-2′-deoxyguanosine concentrations, and serum redox status in persons exposed to mercury. Clinical Chemistry 51, 759–767.

Chen, J., Han, C.-M., Lin, X.-W., Tang, Z.-J., Su, S.-J., 2006. Effect of silver nanoparticle dressing on second degree burn wound. Zhonghua Wai Ke Za Zhi 44, 50–52.

Cheng, L.-C., Jiang, X., Wang, J., Chen, C., Liu, R.-S., 2013. Nano-bio effects: interaction of nanomaterials with cells. Nanoscale 5, 3547–3569.

Chithrani, B.D., Chan, W.C.W., 2007. Elucidating the mechanism of cellular uptake and removal of protein-coated gold nanoparticles of different sizes and shapes. Nano Letters 7, 1542–1550.

Chithrani, B.D., Stewart, J., Allen, C., Jaffray, D.A., 2009. Intracellular uptake, transport, and processing of nanostructures in cancer cells. Nanomedicine – Nanotechnology 5, 118–127.
Cohen, M.S., Stern, J.M., Vanni, A.J., Kelley, R.S., Baumgart, E., Field, D., Libertino, J.A., Summerhayes, I.C., 2007. In vitro analysis of a nanocrystalline silver-coated surgical mesh. Surgical Infections 8, 397–404.
Dwivedi, S., Saquib, Q., Al-Khedhairy, A.A., Musarrat, J., 2012. Butachlor induced dissipation of mitochondrial membrane potential, oxidative DNA damage and necrosis in human peripheral blood mononuclear cells. Toxicology 302, 77–87.
Fenech, M., 2006. Cytokinesis-block micronucleus assay evolves into a "cytome" assay of chromosomal instability, mitotic dysfunction and cell death. Mutation Research – Fundamental and Molecular Mechanisms of Mutagenesis 600, 58–66.
Fenech, M., 2007. Cytokinesis-block micronucleus cytome assay. Nature Protocols 2, 1084–1104.
Flower, N., Brabu, B., Revathy, M., Gopalakrishnan, C., Raja, S., Murugan, S., Kumaravel, T., 2012. Characterization of synthesized silver nanoparticles and assessment of its genotoxicity potentials using the alkaline comet assay. Mutation Research – Genetic Toxicology and Environmental Mutagenesis 742, 61–65.
Foldbjerg, R., Dang, D.A., Autrup, H., 2011. Cytotoxicity and genotoxicity of silver nanoparticles in the human lung cancer cell line, A549. Archives of Toxicology 85, 743–750.
Foldbjerg, R., Irving, E., Hayashi, Y., Sutherland, D., Thorsen, K., Autrup, H., Beer, C., 2012. Global gene expression profiling of human lung epithelial cells after exposure to nanosilver. Toxicological Sciences 130, 145–157.
Foldbjerg, R., Olesen, P., Hougaard, M., Dang, D.A., Hoffmann, H.J., Autrup, H., 2009. PVP-coated silver nanoparticles and silver ions induce reactive oxygen species, apoptosis and necrosis in THP-1 monocytes. Toxicology Letters 190, 156–162.
Fu, J., Ji, J., Fan, D., Shen, J., 2006. Construction of antibacterial multilayer films containing nanosilver via layer-by-layer assembly of heparin and chitosan-silver ions complex. Journal of Biomedical Materials Research A 79, 665–674.
Hackenberg, S., Scherzed, A., Kessler, M., Hummel, S., Technau, A., Froelich, K., Ginzkey, C., Koehler, C., Hagen, R., Kleinsasser, N., 2011. Silver nanoparticles: evaluation of DNA damage, toxicity and functional impairment in human mesenchymal stem cells. Toxicology Letters 201, 27–33.
Hayashi, Y., Engelmann, P., Foldbjerg, R., Szabó, M., Somogyi, I., Pollák, E., Molnár, L., Autrup, H., Sutherland, D.S., Scott-Fordsmand, J., 2012. Earthworms and humans in vitro: characterizing evolutionarily conserved stress and immune responses to silver nanoparticles. Environmental Science & Technology 46, 4166–4173.
Hsin, Y.H., Chen, C.F., Huang, S., Shih, T.S., Lai, P.S., Chueh, P.J., 2008. The apoptotic effect of nanosilver is mediated by a ROS-and JNK-dependent mechanism involving the mitochondrial pathway in NIH3T3 cells. Toxicology Letters 179, 130–139.
Ishikawa, K., Ishii, H., Saito, T., 2006. DNA damage-dependent cell cycle checkpoints and genomic stability. DNA Cell Biology 25, 406–411.
Karlsson, H.L., Gustafsson, J., Cronholm, P., Möller, L., 2009. Size-dependent toxicity of metal oxide particles – a comparison between nano-and micrometer size. Toxicology Letters 188, 112–118.
Kasai, H., 1997. Analysis of a form of oxidative DNA damage, 8-hydroxy-2'-deoxyguanosine, as a marker of cellular oxidative stress during carcinogenesis. Mutation Research 387, 147–163.
Kim, S., Choi, J.E., Choi, J., Chung, K.H., Park, K., Yi, J., Ryu, D.Y., 2009. Oxidative stress-dependent toxicity of silver nanoparticles in human hepatoma cells. Toxicology in Vitro 23, 1076–1084.
Kim, T.H., Kim, M., Park, H.S., Shin, U.S., Gong, M.S., Kim, H.W., 2012. Size-dependent cellular toxicity of silver nanoparticles. Journal of Biomedical Materials Research Part A 100, 1033–1043.
Kim, H.R., Kim, M.J., Lee, S.Y., Oh, S.M., Chung, K.H., 2011. Genotoxic effects of silver nanoparticles stimulated by oxidative stress in human normal bronchial epithelial (BEAS-2B) cells. Mutation Research–Genetic Toxicology and Environmental Mutagenesis 726, 129–135.
Kim, Y.S., Kim, J.S., Cho, H.S., Rha, D.S., Kim, J.M., Park, J.D., Choi, B.S., Lim, R., Chang, H.K., Chung, Y.H., 2008. Twenty-eight-day oral toxicity, genotoxicity, and gender-related tissue distribution of silver nanoparticles in Sprague-Dawley rats. Inhalation Toxicology 20, 575–583.
Kittler, S., Greulich, C., Diendorf, J., Koller, M., Epple, M., 2010. Toxicity of silver nanoparticles increases during storage because of slow dissolution under release of silver ions. Journal of Materials Chemistry 22, 4548–4554.
Lao, F., Chen, L., Li, W., Ge, C., Qu, Y., Sun, Q., Zhao, Y., Han, D., Chen, C., 2009a. Fullerene nanoparticles selectively enter oxidation-damaged cerebral microvessel endothelial cells and inhibit JNK-related apoptosis. ACS Nano 3, 3358–3368.
Lao, F., Li, W., Han, D., Qu, Y., Liu, Y., Zhao, Y., Chen, C., 2009b. Fullerene derivatives protect endothelial cells against NO-induced damage. Nanotechnology 20, 225103.
Li, Y., Liu, Y., Fu, Y., Wei, T., Le Guyader, L., Gao, G., Liu, R.-S., Chang, Y.-Z., Chen, C., 2012. The triggering of apoptosis in macrophages by pristine graphene through the MAPK and TGF-beta signaling pathways. Biomaterials 33, 402ndash411.
Lima, R., Seabra, A.B., Duran, N., 2012. Silver nanoparticles: a brief review of cytotoxicity and genotoxicity of chemically and biogenically synthesized nanoparticles. Journal of Applied Toxicology 32, 867–879.
Liu, J., Hurt, R.H., 2010. Ion release kinetics and particle persistence in aqueous nano-silver colloids. Environmental Science & Technology 44, 2169–2175.
Liu, Y., Li, W., Lao, F., Liu, Y., Wang, L., Bai, R., Zhao, Y., Chen, C., 2011. Intracellular dynamics of cationic and anionic polystyrene nanoparticles without direct interaction with mitotic spindle and chromosomes. Biomaterials 32, 8291–8303.
Lubick, N., 2008. Nanosilver toxicity: ions, nanoparticles or both? Environmental Science & Technology 42, 8617.
Meng, L., Jiang, A., Chen, R., Li, C., Wang, L., Qu, Y., Wang, P., Zhao, Y., Chen, C., 2012. Inhibitory effects of multiwall carbon nanotubes with high iron impurity on viability and neuronal differentiation in cultured PC12 cells. Toxicology http://dx.doi.org/10.1016/j.tox.2012.1011.1011
Midander, K., Cronholm, P., Karlsson, H.L., Elihn, K., Möller, L., Leygraf, C., Wallinder, I.O., 2009. Surface characteristics copper release, and toxicity of nano-and micrometer-sized copper and copper (II) oxide particles: a cross-disciplinary study. Small 5, 389–399.
Mosmann, T., 1983. Rapid colorimetric assay for cellular growth and survival: application to proliferation and cytotoxicity assays. Journal of Immunological Methods 65, 55–63.
Musarrat, J., Arezina-Wilson, J., Wani, A., 1996. Prognostic and aetiological relevance of 8-hydroxyguanosine in human breast carcinogenesis. European Journal of Cancer 32, 1209–1214.
Nielsen, P.S., De Pater, N., Okkels, H., Autrup, H., 1996. Environmental air pollution and DNA adducts in Copenhagen bus drivers – effect of GSTM1 and NAT2 genotypes on adduct levels. Carcinogenesis 17, 1021–1027.
OECD, 2013. Guidelines for the Testing of Chemicals Test No. 487: In Vitro Mammalian Cell Micronucleus Test.
Olinski, R., Gackowski, D., Rozalski, R., Foksinski, M., Bialkowski, K., 2003. Oxidative DNA damage in cancer patients: a cause or a consequence of the disease development? Mutation Research – Fundamental and Molecular Mechanisms of Mutagenesis 531, 177–190.
Park, E.J., Yi, J., Kim, Y., Choi, K., Park, K., 2010. Silver nanoparticles induce cytotoxicity by a Trojan-horse type mechanism. Toxicology in Vitro 24, 872–878.
Peckys, D.B., de Jonge, N., 2011. Visualizing gold nanoparticle uptake in live cells with liquid scanning transmission electron microscopy. Nano Letters 11, 1733–1738.
Porter, A.E., Muller, K., Skepper, J., Midgley, P., Welland, M., 2006. Uptake of C60 by human monocyte macrophages, its localization and implications for toxicity: studied by high resolution electron microscopy and electron tomography. Acta Biomaterials 2, 409–419.
Raoof, M., Mackeyev, Y., Cheney, M.A., Wilson, L.J., Curley, S.A., 2012. Internalization of C60 fullerenes into cancer cells with accumulation in the nucleus via the nuclear pore complex. Biomaterials 33, 2952–2960.
Samuel, U., Guggenbichler, J., 2004. Prevention of catheter-related infections: the potential of a new nano-silver impregnated catheter. International Journal of Antimicrobial Agents 23, 75–78.
Singh, R., Teichert, F., Verschoyle, R.D., Kaur, B., Vives, M., Sharma, R.A., Steward, W.P., Gescher, A.J., Farmer, P.B., 2009. Simultaneous determination of 8-oxo-2′-deoxyguanosine and 8-oxo-2′-deoxyadenosine in DNA using online column-switching liquid chromatography/tandem mass spectrometry. Rapid Communications in Mass Spectrometry 23, 151–160.
Toduka, Y., Toyooka, T., Ibuki, Y., 2012. Flow cytometric evaluation of nanoparticles using side-scattered light and reactive oxygen species-mediated fluorescence-correlation with genotoxicity. Environmental Science & Technology 46, 7629–7636.
Van Engeland, M., Ramaekers, F.C., Schutte, B., Reutelingsperger, C.P., 1996. A novel assay to measure loss of plasma membrane asymmetry during apoptosis of adherent cells in culture. Cytometry 24, 131–139.
Wang, L., Liu, Y., Li, W., Jiang, X., Ji, Y., Wu, X., Xu, L., Qiu, Y., Zhao, K., Wei, T., 2010. Selective targeting of gold nanorods at the mitochondria of cancer cells: implications for cancer therapy. Nano Letters 11, 772–780.
Wei, L., Tang, J., Zhang, Z., Chen, Y., Zhou, G., Xi, T., 2010. Investigation of the cytotoxicity mechanism of silver nanoparticles in vitro. Biomedical Materials 5, 044103.
Xu, X., Yang, Q., Bai, J., Lu, T., Li, Y., Jing, X., 2008. Fabrication of biodegradable electrospun poly(L-lactide-co-glycolide) fibers with antimicrobial nanosilver particles. Journal of Nanoscience and Nanotechnology 8, 5066–5070.
Yang, H., Liu, C., Yang, D., Zhang, H., Xi, Z., 2008. Comparative study of cytotoxicity, oxidative stress and genotoxicity induced by four typical nanomaterials: the role of particle size, shape and composition. Journal of Applied Toxicology 29, 69–78.
Zhao, F., Zhao, Y., Liu, Y., Chang, X., Chen, C., 2011. Cellular uptake, intracellular trafficking, and cytotoxicity of nanomaterials. Small 7, 1322–1337.
Zhou, H., Zhao, K., Li, W., Yang, N., Liu, Y., Chen, C., Wei, T., 2012. The interactions between pristine graphene and macrophages and the production of cytokines/chemokines via TLR-and NF-κB-related signaling pathways. Biomaterials 33, 6933–6942.